Science of the Total Environment 723 (2020) 138160

Contents lists available at ScienceDirect

Science of the Total Environment

journal homepage: www.elsevier.com/locate/scitotenv

Enhanced formation of carbonaceous and nitrogenous disinfection byproducts from biofilm extracellular polymeric substances undercatalysis of copper corrosion products

Jun Hu [a,*], Chen Wang [a], Bijuan Shao [b], Lingxiao Fu [c], Jianming Yu [a], Zhimin Qiang [a,d], Jianmeng Chen [a,*]

[a] College of Environment, Zhejiang University of Technology, 18 Chao-wang Road, Hangzhou 310014, China
[b] Report Department, Zhejiang Fenghe Detection Technology Co., Ltd., 337 Wang-dao Road, Jinhua 322000, China
[c] Faculty of Environmental Engineering, University of Kitakyushu, 1-1 Hibikino, Wakamatsu, Kitakyushu, Fukuoka 8080135, Japan
[d] Key Laboratory of Drinking Water Science and Technology, Research Center for Eco-Environmental Sciences, University of Chinese Academy of Sciences, Chinese Academy of Sciences, 18 Shuang-qing Road, Beijing 100085, China

HIGHLIGHTS

- Copper corrosion products notably enhanced the formation of C-DBPs and N-DBPs.
- The enhancement increased with increasing pH and decreased in the presence of Br^-.
- EPS proteins as a precursor had a higher enhancement than EPS polysaccharides.
- Tyrosine presented the highest enhancement of THMs formation.
- Histidine showed the highest enhancement of HAAs, HANs and HAcAms formation.

GRAPHICAL ABSTRACT

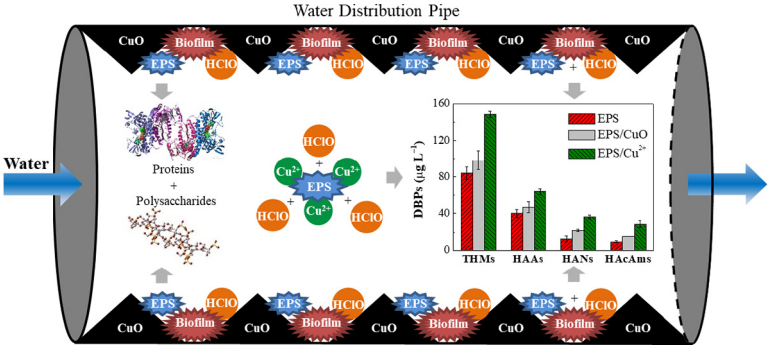

ARTICLE INFO

Article history:
Received 5 January 2020
Received in revised form 22 March 2020
Accepted 22 March 2020
Available online 23 March 2020

Editor: Ching-Hua Huang

Keywords:
Copper corrosion products
Extracellular polymeric substances
Proteins
Polysaccharides
Disinfection byproducts

ABSTRACT

Biofilm formation is ubiquitous on the corroded inner surface of water distribution pipes. Extracellular polymeric substances (EPS) secreted by biofilm microorganisms are nonnegligible precursors of disinfection byproducts (DBPs). The aim was to study the catalysis of copper corrosion products (CCPs, CuO and Cu^{2+}) on the formation of carbonaceous and nitrogenous DBPs (C-DBPs and N-DBPs) with EPS as a precursor. Results indicate that CCPs had a remarkable enhancement on the formation of DBPs, especially N-DBPs. The enhancement by Cu^{2+} was mainly via homogeneous catalysis initiating from its complexation with EPS, while that by CuO was primarily through heterogeneous catalysis initiating from the polarization of Cl atom in HOCl/OCl^-. The enhancement was more evident as pH increased because an alkaline condition favored the electrostatic interactions of CCPs with EPS and HOCl/OCl^-. The presence of Br^- weakened the enhancement, which may be attributed to that HOBr/OBr^- had a much higher reaction rate than HOCl/OCl^- towards the low reactive moieties in EPS. Due to more phenolic or unsaturated/conjugated groups, EPS proteins had a higher catalytic formation of DBPs than EPS polysaccharides. Among the major amino acids in EPS proteins for DBPs formation, tyrosine had the highest enhancement on the formation of trihalomethanes, while histidine had the highest catalytic formation of halogenated acetic acids, acetonitriles and acetamides. The study helps to understand the formation of DBPs by the joint actions of EPS and CCPs in drinking water distribution systems.

* Corresponding authors.
E-mail addresses: hujun1988@zjut.edu.cn (J. Hu), jchen@zjut.edu.cn (J. Chen).

https://doi.org/10.1016/j.scitotenv.2020.138160
0048-9697/

1. Introduction

High doses of residual chlorine are widely used to maintain the microbial stability in drinking water distribution systems (DWDSs) (LeChevallier et al., 1988). However, the microbial control by this means may seriously deteriorate water quality due to the enhanced formation of disinfection byproducts (DBPs) via a series of reactions among precursors, chlorine and pipe corrosion products (PCPs). In the previous studies with regard to the effects of PCPs on DBPs formation (Lin et al., 2008; Gallard et al., 2009; Liu and Croue, 2016), the precursors were primarily focused on natural organic matter (NOM), while biofilm extracellular polymeric substances (EPS) were largely ignored.

Biofilm formation is ubiquitous in DWDSs because of the continuous feeding of unremoved NOM. The EPS secreted by biofilm makes up >80% of hydrated biofilm, and composes of various biomolecules, such as proteins and polysaccharides (Wingender et al., 1999). These biomolecules are usually rich in nitrogen and have a smaller molecular weight than NOM, thus the rate and species of DBPs formation are greatly different (Wang et al., 2013). It was frequently reported that the biomolecules derived from aquatic organisms has a great health risk because of a higher toxicity of nitrogenous DBPs (N-DBPs) than carbonaceous DBPs (C-DBPs) (Lee et al., 2007; Richardson et al., 2007; Hong et al., 2008; Fang et al., 2010). Recently, Wang et al. (2012, 2013) investigated the impacts of EPS and the components on the formation of C-DBPs and N-DBPs, and proposed that biofilm is a nonnegligible precursor of DBPs and its elimination should be seriously considered. However, no literature reported the DBPs formation with biofilm EPS as precursors under the catalysis of PCPs.

Copper has been widely applied in water distribution pipes due to the inactivation of copper ions on certain bacterial species (Feng et al., 1996). The corrosion of copper pipes produces cupric oxide (CuO) on the inner surface and releases cupric ions (Cu^{2+}) into drinking water (Li et al., 2007). It is well known that copper corrosion products (CCPs) can significantly catalyze the formation of DBPs (Zhang and Andrews, 2012; Hu et al., 2016; Liu and Croue, 2016). Hu et al. (2016) found that both Cu^{2+} and CuO accelerated the formation of brominated DBPs (Br-DBPs) during the chlorination of Br^--containing waters, with increasing ratios (IRs) of 50.1% and 7.1%, respectively. Liu and Croue (2016) investigated the CuO-catalyzed formation of DBPs during the chlorination of six organic isolates, and drew a conclusion that the enhancement was more likely to occur with the low-$SUVA_{254}$ isolates, indicating that the precursors had an important impact on the catalysis of CuO.

In this paper, biofilm EPS was applied as a precursor to study the catalysis of two CCPs (CuO and Cu^{2+}) on the formation of DBPs (trihalomethanes, THMs; haloacetic acids, HAAs; haloacetonitriles, HANs; haloacetamides, HAcAms) (Text S1). Despite previous findings, this research mainly focused on: 1) illustrating the enhancement on the formation of C– and N-DBPs from EPS; 2) clarifying the contributions of two EPS components (EPS proteins and polysaccharides) to the catalytic formation of DBPs; 3) revealing the catalytic mechanism of C– and N-DBPs formation from major protein monomers (amino acids). This study helps to comprehensively understand the DBPs formation under the joint actions of EPS and CCPs, and develop the corresponding control strategies when biofilm outbreaks in DWDSs.

2. Materials and methods

2.1. Chemicals

CuO particles were prepared by the CTAB-assisted hydrothermal method with a pH_{PZC} (pH at the point of zero charge) and specific surface area of 8.3 and 12.8 $m^2\ g^{-1}$, respectively (Text S2) (Liu et al., 2012). HOCl, Br^- and Cu^{2+} were spiked in the forms of NaOCl solution (>10%, w/w), KBr and $Cu(NO_3)_2$ (Sinopharm Chemical Reagent, Shanghai), respectively. To prepare stock solution, humic acid (HA) solids (Aladdin, Shanghai) was dissolved into Milli-Q water and filtered through 0.45-μm membrane filters. Biofilm was scraped carefully from the surface of corrosion scales in a water distribution pipe used for 20 years (Hangzhou) and cultivated with a Luria-Bertani medium after rapidly transporting into laboratory within 2 h. Cultures were harvested at the late exponential phase, centrifuged at 2000 rpm for 20 min, and then rinsed with phosphate buffer (1.0 mM, pH 7.0) for 3 times to remove excessive media. EPS were extracted from the obtained cultures by the cation exchange resin method (Frølund et al., 1996). EPS polysaccharides and proteins were extracted by the modified ethanol and trichloroacetic acid precipitation method, respectively (Text S3) (Silva et al., 2012; Zhang et al., 2015). Twenty amino acids (Sangon Biotech, Shanghai, China) included alanine (Ala), arginine (Arg), asparagine (Asn), aspartic acid (Asp), tryptophan (Trp) cysteine (Cys), glutamic acid (Glu), glutamine (Gln), glycine (Gly), histidine (His), isoleucine (Ile), leucine (Leu), lysine (Lys), methionine (Met), phenylalanine (Phe), proline (Pro), serine (Ser), threonine (Thr), tyrosine (Tyr) and valine (Val) (Table S1).

2.2. Analytical methods

THMs, HANs and HAcAms were extracted by the modified EPA Method 551.1, and HAAs were extracted by the modified EPA Method 552.3 (USEPA, 1995, 2003). All the DBPs were analyzed by a gas chromatograph coupled with an electron capture detector (GC/ECD) (Agilent 6890 N) and DB-5 m separation column (30 m × 0.25 mm, 0.25 μm). Various quality control (QC) measures were undertaken to ensure analytical precision and accuracy. All the details were described in Text S4.

Chlorine was quantified by the *N, N*-diethyl-*p*-phenylenediamine method (Rice, 2012). Br^- concentration was measured by an ion chromatograph (Dionex-ICS2000) equipped with an Ionpac AS19 column (250 mm × 4.0 mm, 5.0 μm). KOH solution was used as an eluent at a concentration and flow rate of 20 mM and 1.0 mL min^{-1}, respectively. Total organic carbon (TOC) and total nitrogen (TN) was quantified by a TOC–L_{CPH} analyzer (Shimadzu). The specific surface area of CuO was measured by a TriStar II 3020 surface area and porosity analyzer (Micromeritics). The pHpzc of CuO particles was determined by a potentiometric titration (Liu et al., 2012).

2.3. Reaction system

Brown bottles for reaction (250 mL) were made chlorine demand free before use. All experiments were conducted under magnetic agitation at ambient temperature (25 ± 2 °C). The reaction pH was buffered with borate (1.0 mM) and adjusted by NaOH or HNO_3 solution. To clearly observe the catalysis of CCPs, the doses of chlorine and EPS were increased accordingly to 5.0 mg C L^{-1} and 9.8 mg Cl_2 L^{-1}, respectively (Liu et al., 2017; Wang et al., 2013). For the same reason, the dose of CuO and Cu^{2+} were chosen at relatively higher levels in the previous studies on drinking water (Li et al., 2007; Zhang and Andrews, 2012; Hu et al., 2016), namely, 2.0 g L^{-1} and 2.0 mg L^{-1}, respectively. Water samples were withdrawn after preselected time intervals, rapidly filtered through 0.45-μm membrane filters, and then quickly spiked with an excess of ascorbic acid to quench the residual chlorine (>0.3 mg Cl_2 L^{-1}). As shown in Fig. S1, DBPs were formed rapidly within 24 h and scarcely after 48 h, thus the reaction time was set at 72 h to ensure a stable stage of DBPs formation. All the experiments were performed in duplicate and the mean values of data were used only if relative percent differences (RPDs) were <20%.

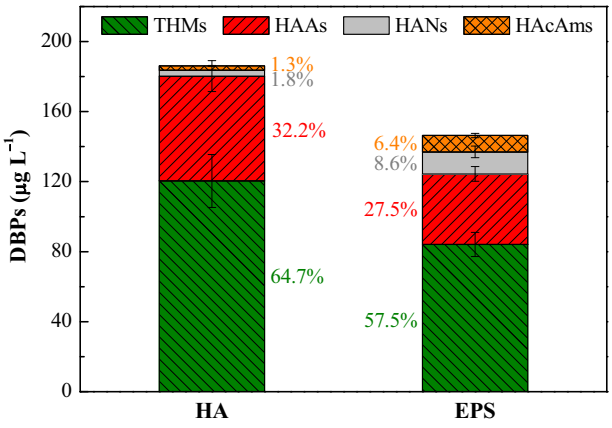

Fig. 1. Formation of carbonaceous and nitrogenous disinfection byproducts (C-DBPs and N-DBPs) from humic acid (HA) and extracellular polymeric substances (EPS) in the absence of copper corrosion products. Experimental conditions: $[Cl_2]_0 = 9.8$ mg L^{-1}, $[HA]_0 = [EPS]_0 = 5.0$ mg C L^{-1}, pH = 7.6, reaction time = 72 h. Error bars represent the relative percent differences (RPDs, $n = 2$).

3. Results and discussion

3.1. Catalytic formation of DBPs from biofilm EPS

Batch experiments were performed to elucidate the DBPs formation with HA and EPS (5 mg C L^{-1}) as precursors (Fig. 1). The ratios of carbon to nitrogen (C/N) of HA and EPS were 9.4 and 2.6, respectively. Obviously, HA had a higher DBPs formation potential than EPS, with values of 181.6 and 146.7 μg L^{-1}, respectively. However, for N-DBPs, EPS showed a higher formation potential than HA, which may be attributed to the higher content of N. The N-DBPs formation potentials of EPS and HA were 22.0 and 5.8 μg L^{-1}, accounting for 3.2% and 15.0% of formed DBPs, respectively. It was reported that HANs and HAcAms were nearly 100 times more cytotoxic and 10 times more genotoxic than HAAs in the Chinese hamster ovary cell assays (Muellner et al., 2007; Plewa et al., 2008). Therefore, the health risk posed by biofilm EPS as a precursor cannot be neglected even though its amount is relatively lower than that of NOM in bulk water.

As shown in Fig. 2, both Cu^{2+} and CuO had the enhancement on the formation of DBPs from EPS. For an instance, the IRs of THMs by Cu^{2+} and CuO were 77.0% and 17.1%, respectively. Moreover, CCPs had a higher enhancement on the formation of N-DBPs than C-DBPs. For example, the IRs by Cu^{2+} were 77.0%, 59.0%, 187.1% and 204.6% for

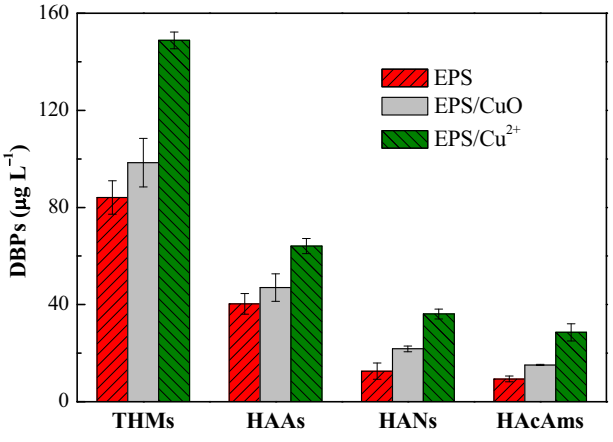

Fig. 2. Catalytic formation of DBPs from EPS. Experimental conditions: $[Cl_2]_0 = 9.8$ mg L^{-1}, $[EPS]_0 = 5.0$ mg C L^{-1}, [CuO] = 2.0 g L^{-1}, $[Cu^{2+}] = 2.0$ mg L^{-1}, pH = 7.6, reaction time = 72 h. Error bars represent the RPDs (n = 2).

THMs, HAAs, HANs and HAcAms formation, respectively. The result further demonstrates that EPS as a precursor deserves more attention in DWDSs.

It has been reported that, with NOM as a precursor, the enhancement by Cu^{2+} was mainly to accelerate the ionization of carbonyl and hydroxyl groups via homogeneous catalysis (Blatchley et al., 2003). However, with EPS as a precursor, the catalysis by Cu^{2+} also occurred though the spontaneous decarboxylation of the complexes (CuOX and $CuHOX^+$, X are carboxyl groups) because the protein components accounted for the most of DBPs formation (Pedersen, 1952; Wang et al., 2013). The heterogeneous catalysis by CuO was mainly initiated from the polarization of Cl atom in HOCl/OCl^-, which had two impacts on the formation of DBPs. On the one hand, the CuO-induced polarization increased the electrophilicity of Cl atom and then accelerated the chlorine substitution reaction, which induced the enhancement on DBPs formation (Liu and Croue, 2016). On the other hand, the CuO-induced polarization greatly promoted the chlorine decay via disproportionation and oxygen generation (Eqs. (1) and (2)) (Liu et al., 2012):

$$3HOCl \xrightarrow{CuO} 2Cl^- + ClO_3^- + 3H^+, k_{ClO} \quad (1)$$

$$2HOCl \xrightarrow{CuO} 2Cl^- + O_2 + 2H^+, k_{ClP} \quad (2)$$

The CuO-catalyzed chlorine decay rate (k_{Cl}, the sum of k_{ClO} and k_{ClP}) achieved 10.8, 9.5 and 2.7 M^{-1} s^{-1} at pHs 6.6, 7.6 and 8.6, respectively. Generally, the reaction rates of HOCl/OCl^- with NOM are lower than 10^2 M^{-1} s^{-1} (Gallard and von Gunten, 2002; Westerhoff et al., 2004). Therefore, the CuO-catalyzed chlorine decay may retard the reaction between HOCl/OCl^- and EPS, reducing the formation of DBPs. Additionally, the organic moieties in EPS were also absorbed on the positively charged CuO surface, which increased their reactivity towards HOCl/OCl^- (Zhang and Andrews, 2012). The net effect came out to be that the presence of CuO facilitated the formation of DBPs.

3.2. Influence factors

3.2.1. pH

The catalytic formation of DBPs from EPS was investigated in the pH range of 6.6–9.6. As shown in Fig. 3, in the absence of CCPs, the formation of THMs, HAAs and HANs decreased with increasing pH, while that of HAcAms maximized at pH 7.6. The specificity of HAcAms was ascribed to a larger difference between the hydrolysis rates of HANs and HAcAms at pH 7.0–8.0 than at other pH levels (Chu et al., 2012). Notably, the catalysis of CCPs was dependent on pH, and the enhancement became more apparent at a higher pH. For an instance, the IR of HAcAms by CuO increased from 28.4% to 72.2% as pH increased from 6.6 to 9.6. On the one hand, a higher pH facilitated the ionization of carboxyl, carbonyl and hydroxyl groups in EPS (Fig. S2) (Pedersen, 1952; Zhang and Andrews, 2012). One the other hand, Cu^{2+} was gradually converted into $Cu(OH)^+$ and $Cu(OH)_2$ as pH increased from 6.6 to 9.6, which induced a weaker positive charge (Plyasunova et al., 1997). The net effect came out to be that a higher pH facilitated the electrostatic interactions between Cu^{2+} and EPS. pH could also impact the catalysis of CuO in the same way that it affected the catalysis of Cu^{2+}. But beyond that, an alkaline pH promoted the deprotonation of HOCl and enhanced the electrostatic interaction between OCl^- and the positively charged CuO surface to form CuO-OCl^- complex, which may facilitate the catalysis of CuO (Liu et al., 2012).

3.2.2. Br^-

Bromine utilization factor (BUF) and bromine incorporation factor (BIF) were applied to investigate the impact of Br^- on the catalytic formation of DBPs from EPS. BUF refers to the percentage of Br^- utilized in forming Br-DBPs, while BIF refers to the proportion of Br-DBPs partially or totally substituted by Br (Text S5) (Chu et al., 2013). In the absence of

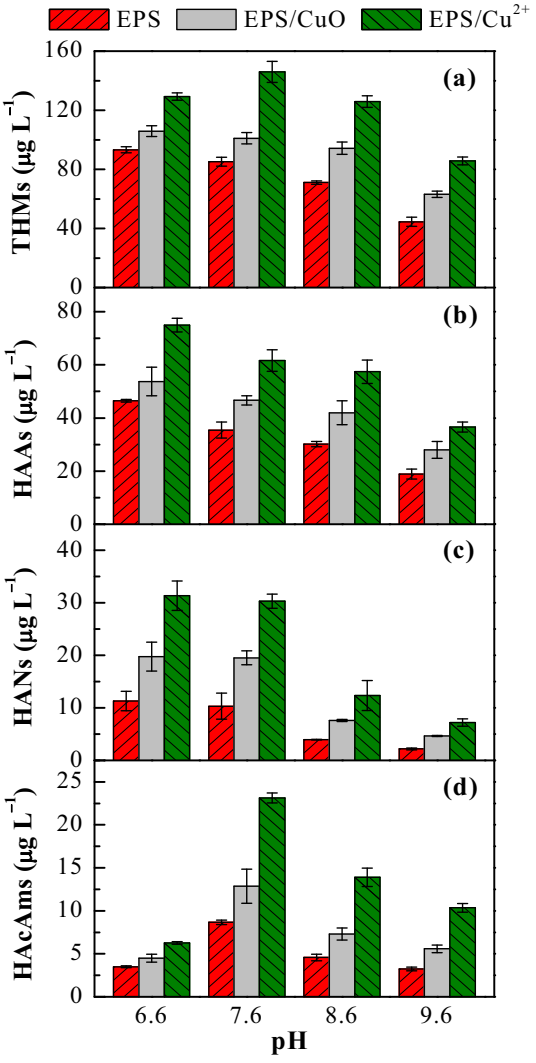

Fig. 3. Effect of pH on the catalytic formation of DBPs from EPS. Experimental conditions: $[Cl_2]_0 = 9.8$ mg L^{-1}, $[EPS]_0 = 5.0$ mg C L^{-1}, [CuO] = 2.0 g L^{-1}, $[Cu^{2+}] = 2.0$ mg L^{-1}, reaction time = 72 h. Error bars represent the RPDs (n = 2).

CCPs, the BUFs and BIFs of C-DBPs were higher than those of N-DBPs, implying that a large fraction of Br was incorporated into the precursors of C-DBPs (Fig. 4). As expected, in the presence of CCPs, both BUF and BIF values presented an upward trend, especially for C-DBPs. For example, the BUF and BIF of THMs with Cu^{2+} increased from 0.11 to 0.15 and 1.59 to 2.02, respectively. The result indicates that CCPs shifted the formed DBPs from chlorinated to multiple brominated species. However, the enhancement by CCPs in the presence of Br^- was much weaker than that in the absence of Br^-. For an instance, the IRs of HAcAms by CuO were 25.7% and 61.1% with and without Br^-, respectively (Figs. 1 and 4). The catalysis of CCPs was achieved by the acceleration of the reactions between oxidants and the low reactive moieties (Liu and Croue, 2016). The consumption oxidant involves two-stage reaction kinetics (rapid initial and slow continuous stages). During the slow stage, the second-order rate constants of $HOBr/OBr^-$ were approximately 20–30 times those of $HOCl/OCl^-$ towards the low reactive moieties, with values of 15–167 and 0.7–5 M^{-1} s^{-1}, respectively (Westerhoff et al., 2004). Moreover, at pH 7.6, the fraction of OCl^- in $HOCl/OCl^-$ (ca. 50%) is higher than that of OBr^- in $HOBr/OBr^-$ (ca. 10%). Therefore, without CCPs, the DBPs formation in the presence of Br^- was much higher than that in the absence of Br^-. The decreased IRs may be attributed to that, after the addition of Br^-, the enhanced DBPs formation by CCPs did not increase accordingly with the increasing DBPs formation without CCPs due to the limitation of precursor dose. In a word, it was more likely for CCPs to achieve a higher enhancement by accelerating the reactions of $HOCl/OCl^-$ with the low reactive moieties in EPS.

3.3. Catalytic formation of DBPs from EPS proteins and polysaccharides

Proteins and polysaccharides were reported as the major components (ca. 80%) of EPS (Comte et al., 2006), thus the two biomolecules were extracted and employed as precursors to further elucidate the catalysis of CCPs. Without CCPs, polysaccharides presented a lower formation potential of DBPs than proteins due to the higher content of saturated carbon ring structures (Fig. 5). Wang et al. (2013) reported that the major precursors of DBPs were the compounds with unsaturated/conjugated carbon bonds or phenolic structures. The polysaccharide monomers in EPS mainly consist of galactose, glucosamine, glucose, glucuronic acid, rhamnose and mannose, but only glucosamine contains organic nitrogen, which resulted in little formation of N-DBPs (<2.0 μg L^{-1}) (Wingender et al., 1999). The catalytic formation of DBPs from polysaccharides was also much lower than that from proteins. For an instance, the IRs of THMs by Cu^{2+} from proteins and polysaccharides were 97.3% and 20.8%, respectively. The phenolic or unsaturated/conjugated structures in proteins were more capable for withdrawing electrons from α-carbons than the saturated carbon ring structures in polysaccharides. As a result, a higher electron density was beneficial to the complexation of proteins with Cu^{2+} and the positively charged CuO surface. However, Liu and Croue (2016) found that the enhancement by CuO from low reactive NOM isolates (with fulvic

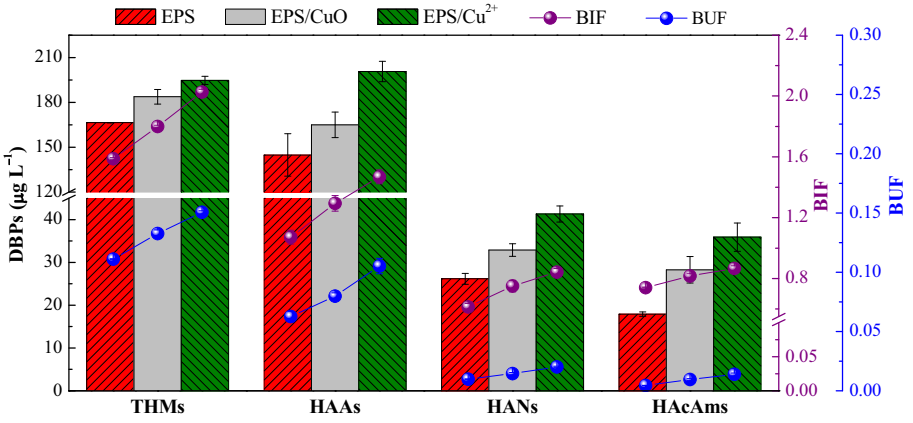

Fig. 4. Effect of Br^- on the catalytic formation of DBPs from EPS. Experimental conditions: $[Cl_2]_0 = 9.8$ mg L^{-1}, $[EPS]_0 = 5.0$ mg C L^{-1}, [CuO] = 2.0 g L^{-1}, $[Cu^{2+}] = 2.0$ mg L^{-1}, $[Br^-]_0 = 1.0$ mg L^{-1}, pH = 7.6, reaction time = 72 h. Error bars represent the RPDs (n = 2).

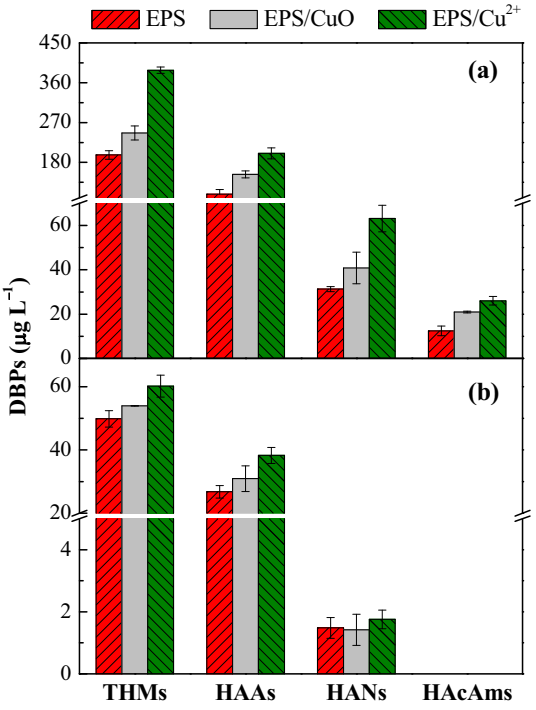

Fig. 5. Catalytic formation of DBPs from EPS proteins (a) and polysaccharides (b). Experimental conditions: $[Cl_2]_0$ = 9.8 mg L^{-1}, $[Proteins]_0$ = $[Polysaccharides]_0$ = 5.0 mg C L^{-1}, [CuO] = 2.0 g L^{-1}, $[Cu^{2+}]$ = 2.0 mg L^{-1}, pH = 7.6, reaction time = 72 h. Error bars represent the RPDs (n = 2).

acid structures incorporating abundant polysaccharide moieties) was much higher than that from active ones (with more aromatic/phenolic structures and carboxyl groups) during chlorination of Br^--containing waters. The difference may be owed to the generation of HOBr/OBr^-, which reacts with NOM at a rate of 10 times faster than HOCl/OCl^- (Westerhoff et al., 2004). In this study, the presence of Br^- significantly weakened the enhancement because of the higher reaction rate of HOBr/OBr^- with the low reactive moieties in EPS (possibly polysaccharides).

3.4. Catalytic formation of DBPs from amino acids

CCPs mainly catalyzed EPS proteins to form DBPs, thus the species and contents of amino acids were analyzed. Twenty amino acids were identified, which accounted for 99% of EPS proteins (Table S1). To study the effect of their chemical structure on the catalysis of CCPs, the identified amino acids were added separately as precursors at a concentration (3.0 mg C L^{-1}). Without CCPs, Trp and Tyr had a quite high THMs formation potential with values of 314.8 and 150.5 μg L^{-1}, respectively, while Asn, Asp, His, Trp and Tyr had a quite high HAAs formation potential with values of 80.2, 187.1, 102.2, 261.9 and 254.2 μg L^{-1}, respectively (Table 1). Considering the contents of amino acids in EPS proteins, Tyr and Asp primarily contributed to the formation of THMs and HAAs, respectively. The major precursors of HANs and HAcAms were similar, namely Ala, Asn, Asp, His, Trp and Tyr. Thereinto, Ala had a high formation potential of N-DBPs in the absence of CCPs, which was only slightly lower than Asn. Furthermore, Ala accounted for the largest fraction (12.0%) of EPS proteins, thus Ala was considered as the most important precursor of N-DBPs. The results consist with previous studies concerning the DBPs formation from amino acids despite of different reaction conditions (Ueno et al., 1996; Hong et al., 2009; Chu et al., 2010a; Yang et al., 2012). Based on the above, the impact of chemical structure on catalysis was focused on the five major DBP precursors, namely, Asn, Asp, His, Trp and Tyr. The proposed mechanism of enhancement is shown in Fig. 6.

For THMs formation, the enhancement from Tyr was higher than that from Trp. For example, the IRs of THMs by Cu^{2+} from Tyr and Trp were 61.9% and 12.9%, respectively. It was reported that the decarboxylation and chlorine substitution of Tyr successively generated 4-hydroxyl-benzyl-cyanide (4-HBC) and 2,4,6-trichlorophenol (2,4,6-TCP). The opening of benzene ring in 2,4,6-TCP was a main pathway of THMs formation (Chu et al., 2012). As the atomic potential map of Trp shown in Fig. S3, the ruptures of C_2-C_3 and C_4-C_7 bonds (decarboxylation and chlorine substitution) were easier to occur, forming 2-(indol-3-yl)-cyanide (2-IAN) and 2-indole-chloride (2-IC), respectively. The subsequent break of the C_7═C_8 bond in the *penta*-heterocycle was a pivotal step for THMs formation (Li et al., 2019). CCPs may have different capacities to promote the cleavage of the benzene ring in 2,4,6-TCP and the *penta*-heterocycle in 2-IC. First, the N atom in 2-IC has fewer lone pairs of electrons than the O atom in 2,4,6-TCP (Devi and Krishnaiah, 1999; Wendt et al., 2010). Second, the N atom in the *penta*-heterocycle can donate its lone-pair electrons to form *p*–π conjugation with the π electrons of C_7═C_8 bond except the adjacent benzene ring (Shaji et al., 2004). The relatively lower electron density around N atom was not beneficial to its complexation with CCPs, thus weakening the catalysis of CCPs.

For HAAs formation, His showed the highest enhancement among the five amino acids under the catalysis of CCPs. For an instance, the IRs of HAAs by Cu^{2+} from His, Asn, Asp, Trp and Tyr were 39.5%, 27.7%, 18.8%, 22.3% and 21.6%, respectively. It was reported that HAAs formed mainly via decarboxylation, chlorine substitution and the elimination of variable (R′) group (Hureiki et al., 1994; Hong et al., 2009; Li et al., 2017). Similar to THMs formation, the capacities of CCPs to promote the elimination of R′ group played a vital role in the enhancement on HAAs formation. The electrons in R′ group were shifted by CCPs on account of complexation, which promoted the break of C—R′ bond. Two active sites were available for complexation (—N═ and —N—) in the imidazole *penta*-heterocycle of His, whereas only one active site is available in the R′ group of each of other four amino acids (—COOH, —$CONH_2$, —OH or —NH—) (Fig. S4). The more active sites in imidazole *penta*-heterocycle were conducive to the promotion of its removal.

For N-DBPs formation, His also showed the highest enhancement among the five amino acids under the catalysis of CCPs. For example, the IRs of HAcAms by Cu^{2+} from His, Asn, Asp, Trp and Tyr were 214.2%, 134.1%, 116.7%, 151.0% and 149.5%, respectively. The consistent results for the enhanced formation of HAAs, HANs and HAcAms from the five amino acids were mainly ascribed to the associated formation pathway. The elimination of R′ group after decarboxylation and chlorine substitution resulted in the formation of HANs, which was further hydrolyzed to form HAcAms and HAAs successively (Hong et al., 2009; Chu et al., 2010b; Shah and Mitch, 2012). Thereby, the promoted elimination of the imidazole *penta*-heterocycle in His by CCPs also enhanced the formation of N-DBPs.

4. Conclusions

This study investigated the catalysis of CCPs (CuO and Cu^{2+}) on the formation of C-DBPs and N-DBPs with biofilm EPS and their components (polysaccharides and proteins) as precursors. The following conclusions are drawn:

- CCPs had a remarkable enhancement on the DBP formation, especially N-DBPs.
- The catalytic formation of both C-DBPs and N-DBPs was highly pH-dependent. The enhancement became more obvious under an alkaline condition.
- CCPs increased the BUF and BIF of DBPs, while the presence of Br^- weakened the enhancement by CCPs.
- The catalytic formation of DBPs from proteins was much higher than that from polysaccharides. Tyr showed the highest enhancement of

Table 1
Catalytic formation of carbonaceous and nitrogenous disinfection byproducts from twenty amino acids after 72 h reaction.[a]

Amino acids[b]	THMs (μg L^{-1})			HAAs (μg L^{-1})			HANs (μg L^{-1})			HAcAms (μg L^{-1})		
	Control	CuO	Cu^{2+}	Control	CuO	Cu^{2+}	Control	CuO	Cu^{2+}	Control	CuO	Cu^{2+}
Ala	11.4 ± 0.3	19.2 ± 3.0	37.6 ± 0.2	1.9 ± 0.1	2.8 ± 0.5	4.1 ± 0.7	44.1 ± 3.5	52.6 ± 2.5	57.2 ± 4.1	10.3 ± 1.3	12.9 ± 0.9	16.7 ± 0.4
Arg	8.3 ± 0.6	13.4 ± 2.1	20.2 ± 2.3	20.8 ± 3.5	30.4 ± 2.8	45.4 ± 1.7	0.5 ± 0.0	2.1 ± 0.1	3.6 ± 0.3	/	/	/
Asn	11.0 ± 0.5	12.7 ± 0.2	19.3 ± 2.4	80.2 ± 2.0	89.2 ± 3.7	102.4 ± 5.3	46.0 ± 9.1	71.4 ± 12.5	110.4 ± 12.4	10.4 ± 1.3	17.2 ± 2.5	24.3 ± 4.2
Asp	21.3 ± 1.8	27.7 ± 0.4	39.2 ± 4.6	187.1 ± 10.9	197.8 ± 4.3	222.2 ± 8.4	10.1 ± 0.8	15.7 ± 1.6	39.3 ± 4.1	2.9 ± 0.4	7.0 ± 0.6	11.2 ± 0.8
Cys	0.3 ± 0.0	1.1 ± 0.1	1.3 ± 0.2	7.1 ± 0.6	10.0 ± 0.6	14.6 ± 1.2	0.5 ± 0.0	1.1 ± 0.1	2.1 ± 0.2	/	/	/
Gln	4.8 ± 0.2	6.2 ± 2.0	8.7 ± 0.4	3.9 ± 0.4	5.3 ± 1.0	8.1 ± 0.4	3.6 ± 0.1	6.3 ± 0.3	10.2 ± 0.8	/	/	/
Glu	16.5 ± 0.0	26.0 ± 6.5	40.6 ± 2.8	10.0 ± 0.5	14.6 ± 0.6	18.9 ± 1.4	1.5 ± 0.0	3.1 ± 0.1	3.1 ± 0.1	/	/	/
Gly	1.2 ± 0.0	1.7 ± 0.1	2.2 ± 0.3	0.2 ± 0.0	0.3 ± 0.1	0.4 ± 0.1	/[c]	/	/	/	/	/
His	15.9 ± 1.8	18.5 ± 1.5	20.0 ± 2.7	102.2 ± 10.5	118.9 ± 4.2	142.6 ± 10.1	35.0 ± 5.1	54.7 ± 13.2	91.2 ± 7.6	8.7 ± 1.3	13.9 ± 2.1	27.8 ± 2.5
Ile	18.9 ± 5.5	30.2 ± 1.6	44.7 ± 3.2	4.3 ± 0.6	6.3 ± 0.2	10.6 ± 1.5	2.6 ± 0.1	4.1 ± 0.1	5.5 ± 0.2	/	/	/
Leu	8.7 ± 3.0	9.7 ± 1.5	11.4 ± 0.8	4.7 ± 0.6	5.3 ± 0.3	6.1 ± 0.2	/	2.1 ± 0.1	3.6 ± 0.2	/	/	/
Lys	10.6 ± 1.7	13.6 ± 3.3	18.2 ± 0.4	17.1 ± 2.4	22.8 ± 2.1	28.1 ± 1.9	/	0.2 ± 0.0	0.4 ± 0.0	/	/	/
Met	5.4 ± 0.9	9.6 ± 0.2	19.5 ± 1.6	6.8 ± 0.5	9.7 ± 0.9	14.9 ± 0.8	2.7 ± 0.2	4.8 ± 0.2	6.3 ± 0.5	/	/	/
Phe	5.3 ± 0.6	6.5 ± 0.1	10.7 ± 1.6	27.1 ± 2.1	38.8 ± 1.4	55.2 ± 4.9	/	/	/	/	/	/
Pro	10.5 ± 2.7	14.3 ± 0.4	22.0 ± 2.4	40.2 ± 2.5	50.9 ± 3.5	81.6 ± 6.2	2.7 ± 0.1	3.6 ± 0.3	5.1 ± 0.2	/	/	/
Ser	1.32 ± 0.04	1.33 ± 0.39	1.60 ± 0.21	1.4 ± 0.1	1.6 ± 0.1	2.1 ± 0.1	/	/	/	/	/	/
Thr	3.4 ± 0.4	4.1 ± 0.5	5.7 ± 0.5	1.1 ± 0.1	2.2 ± 0.4	3.0 ± 0.5	/	/	/	/	/	/
Trp	314.8 ± 22.0	338.5 ± 9.9	355.3 ± 17.9	261.9 ± 5.0	298.3 ± 12.3	320.3 ± 12.2	18.3 ± 3.28	27.9 ± 8.1	42.6 ± 1.6	4.3 ± 1.0	7.8 ± 0.6	10.5 ± 1.3
Tyr	150.5 ± 7.6	181.2 ± 6.5	243.8 ± 25.9	254.2 ± 15.1	276.8 ± 13.0	309.2 ± 13.4	17.2 ± 2.1	23.8 ± 0.2	46.3 ± 0.7	4.2 ± 1.3	6.7 ± 0.7	10.6 ± 1.2
Val	12.6 ± 3.0	20.5 ± 0.1	24.8 ± 5.1	12.5 ± 4.1	20.1 ± 2.2	27.2 ± 3.5	/	/	/	/	/	/

[a] Experimental conditions: $[Cl_2]_0 = 9.8$ mg L^{-1}, [Amino acids]$_0 = 3.0$ mg C L^{-1}, [CuO] = 2.0 g L^{-1}, $[Cu^{2+}] = 2.0$ mg L^{-1}, pH = 7.6.
[b] Abbreviations: alanine (Ala), arginine (Arg), asparagine (Asn), aspartic acid (Asp), cysteine (Cys), glutamine (Gln), glutamic acid (Glu), glycine (Gly), histidine (His), isoleucine (Ile), leucine (Leu), lysine (Lys), methionine (Met), phenylalanine (Phe), proline (Pro), serine (Ser), threonine (Thr), tryptophan (Trp), tyrosine (Tyr), valine (Val).
[c] Not detected.

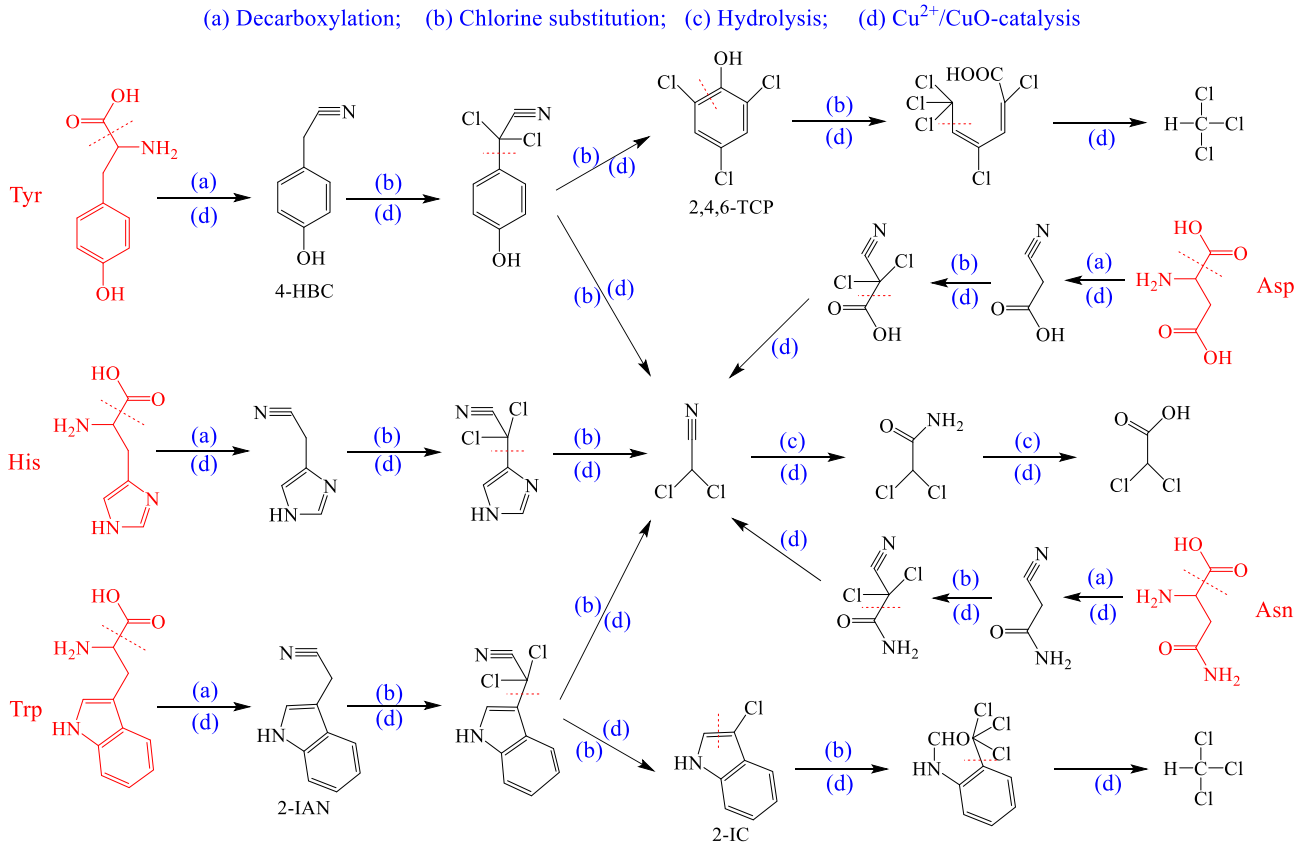

Fig. 6. Proposed mechanism of the catalytic formation of DBPs from amino acids. Experimental conditions: $[Cl_2]_0 = 9.8$ mg L^{-1}, [Amino acids]$_0 = 3.0$ mg C L^{-1}, [CuO] = 2.0 g L^{-1}, $[Cu^{2+}] = 2.0$ mg L^{-1}, pH = 7.6.

THMs formation, while His exhibited the highest enhancement of HAAs, HANs and HAcAms formation.

CRediT authorship contribution statement

Jun Hu: Conceptualization, Investigation, Writing - review & editing. **Chen Wang:**Investigation, Writing - original draft.**Bijuan Shao:**Investigation, Writing - original draft.**Lingxiao Fu:**Resources.**Jianming Yu:** Writing - review & editing.**Zhimin Qiang:**Writing - review & editing. **Jianmeng Chen:**Supervision.

Declaration of competing interest

The authors declare that they have no known competing financial interests or personal relationships that could have appeared to influence the work reported in this paper.

Acknowledgements

This study was financially supported by the National Natural Science Foundation of China (51808496, 51525806), and Special Fund from Key Laboratory of Drinking Water Science and Technology (Research Center for Eco-Environmental Sciences, Chinese Academy of Sciences) (19K03KLDWST).

Appendix A. Supplementary data

Supplementary data to this article can be found online at https://doi.org/10.1016/j.scitotenv.2020.138160.

References

Blatchley, E.R., Margetas, D., Duggirala, R., 2003. Copper catalysis in chloroform formation during water chlorination. Water Res. 37, 4385–4394.
Chu, W.H., Gao, N.Y., Deng, Y., 2010a. Formation of haloacetamides during chlorination of dissolved organic nitrogen aspartic acid. J. Hazard. Mater. 173, 82–86.
Chu, W.H., Gao, N.Y., Deng, Y., Krasner, S.W., 2010b. Precursors of dichloroacetamide, an emerging nitrogenous DBP formed during chlorination or chloramination. Environ. Sci. Technol. 44, 3908–3912.
Chu, W.H., Gao, N.Y., Krasner, S.W., Templeton, M.R., Yin, D.Q., 2012. Formation of halogenated C-, N-DBPs from chlor(am)ination and UV irradiation of tyrosine in drinking water. Environ. Pollut. 161, 8–14.
Chu, W.H., Gao, N.Y., Yin, D.Q., Krasner, S.W., 2013. Formation and speciation of nine haloacetamides, an emerging class of nitrogenous DBPs, during chlorination or chloramination. J. Hazard. Mater. 260, 806–812.
Comte, S., Guibaud, G., Baudu, M., 2006. Biosorption properties of extracellular polymeric substances (EPS) resulting from activated sludge according to their type: soluble or bound. Process Biochem. 41, 815–823.
Devi, L.G., Krishnaiah, G.M., 1999. Photocatalytic degradation of *p*-amino-azo-benzene and *p*-hydroxy-azo-benzene using various heat treated TiO_2 as the photocatalyst. J. Photochem. Photobio. A 121, 141–145.
Fang, J., Ma, J., Yang, X., Shang, C., 2010. Formation of carbonaceous and nitrogenous disinfection by-products from the chlorination of *Microcystis aeruginosa*. Water Res. 44, 1934–1940.
Feng, Y., Teo, W.K., Siow, K.S., Tan, K.L., Hsieh, A.K., 1996. The corrosion behaviour of copper in neutral tap water. Part I: corrosion mechanisms. Corros. Sci. 38, 369–385.
Frølund, B., Palmgren, R., Keiding, K., Nielsen, P.H., 1996. Extraction of extracellular polymers from activated sludge using a cation exchange resin. Water Res. 30, 1749–1758.
Gallard, H., von Gunten, U., 2002. Chlorination of natural organic matter kinetics of chlorination and of THM formation. Water Res. 36, 65–74.
Gallard, H., Allard, S., Nicolau, R., von Gunten, U., Croué, J.P., 2009. Formation of iodinated organic compounds by oxidation of iodide-containing waters with manganese dioxide. Environ. Sci. Technol. 43, 7003–7009.
Hong, H.C., Mazumder, A., Wong, M.H., Liang, Y., 2008. Yield of trihalomethanes and haloacetic acids upon chlorinating algal cells, and its prediction via algal cellular biochemical composition. Water Res. 42, 4941–4948.
Hong, H.C., Wong, M.H., Liang, Y., 2009. Amino acids as precursors of trihalomethane and haloacetic acid formation during chlorination. Arch. Environ. Contam. Toxicol. 56, 638–645.
Hu, J., Qiang, Z.M., Dong, H.Y., Qu, J.H., 2016. Enhanced formation of bromate and brominated disinfection byproducts during chlorination of bromide-containing waters under catalysis of copper corrosion products. Water Res. 98, 302–308.
Hureiki, L., Croue, J.P., Legube, B., 1994. Chlorination studies of free and combined amino acids. Water Res. 28, 2521–2531.
LeChevallier, M.W., Cawthon, C.D., Lee, R.G., 1988. Inactivation of biofilm bacteria. Appl. Environ. Microbiol. 54, 2492–2499.
Lee, W., Westerhoff, P., Croué, J.P., 2007. Dissolved organic nitrogen as a precursor for chloroform, dichloroacetonitrile, *N*-nitrosodimethylamine, and trichloronitromethane. Environ. Sci. Technol. 41, 5485–5490.
Li, B., Qu, J.H., Liu, H.J., Hu, C.Z., 2007. Effects of copper(II) and copper oxides on THMs formation in copper pipe. Chemosphere 68, 2153–2160.
Li, C.J., Gao, N.Y., Chu, W.H., Bond, T., Wei, X.Y., 2017. Comparison of THMs and HANs formation potential from the chlorination of free and combined histidine and glycine. Chem. Eng. J. 307, 487–495.
Li, C., Lin, Q.F., Dong, F.L., Li, Y.H., Luo, F., Zhang, K.J., 2019. Formation of iodinated trihalomethanes during chlorination of amino acid in waters. Chemosphere 217, 355–363.
Lin, Y.P., Washburn, M.P., Valentine, R.L., 2008. Reduction of lead oxide (PbO_2) by iodide and formation of iodoform in the PbO_2/I^-/NOM system. Environ. Sci. Technol. 42, 2919–2924.
Liu, C., Croue, J.P., 2016. Formation of bromate and halogenated disinfection byproducts during chlorination of bromide-containing waters in the presence of dissolved organic matter and CuO. Environ. Sci. Technol. 50, 135–144.
Liu, C., von Gunten, U., Croue, J.P., 2012. Enhanced bromate formation during chlorination of bromide-containing waters in the presence of CuO: catalytic disproportionation of hypobromous acid. Environ. Sci. Technol. 46, 11054–11061.
Liu, L., Hu, Q.Y., Le, Y., Chen, G.W., Tong, Z.L., Xu, Q., Wang, G., 2017. Chlorination-mediated EPS excretion shapes early-stage biofilmformation in drinking water systems. Process Biochem. 55, 41–48.
Muellner, M.G., Wagner, E.D., McCalla, K., Richardson, S.D., Woo, Y.T., Plewa, M.J., 2007. Haloacetonitriles vs. regulated haloacetic acids: are nitrogen-containing DBPs more toxic? Environ. Sci. Technol. 41, 645–651.
Pedersen, K.J., 1952. The uncatalysed and the metal-ion catalysed decarboxylation of oxaloacetic acid. Acta Chem. Scand. 6, 285–303.
Plewa, M.J., Muellner, M.G., Richardson, S.D., Fasano, F., Buettner, K.M., Woo, Y.T., McKague, A.B., Wagner, E.D., 2008. Occurrence, synthesis, and mammalian cell cytotoxicity and genotoxicity of haloacetamides: an emerging class of nitrogenous drinking water disinfection byproducts. Environ. Sci. Technol. 42, 955–961.
Plyasunova, N.V., Wang, M.S., Zhang, Y., Muhammed, M., 1997. Critical evaluation of thermodynamics of complex formation of metal ions in aqueous solutions II. Hydrolysis and hydroxo-complexes of Cu^{2+} at 298.15 K. Hydrometallurgy 45, 37–51.
Rice, E.W., 2012. Standard Methods for the Examination of Water and Wastewater. American Public Health Association, Washington, D.C.
Richardson, S.D., Plewa, M.J., Wagner, E.D., Schoeny, R., Demarini, D.M., 2007. Occurrence, genotoxicity, and carcinogenicity of regulated and emerging disinfection by-products in drinking water: a review and roadmap for research. Mutat. Res. 636, 178–242.
Shah, A.D., Mitch, W.A., 2012. Halonitroalkanes, halonitriles, haloamides, and *N*-nitrosamines: a critical review of nitrogenous disinfection byproduct formation pathways. Environ. Sci. Technol. 46, 119–131.
Shaji, S., Eappen, S.M., Rasheed, T.M.A., Nair, K.P.R., 2004. NIR vibrational overtone spectra of *N*-methylaniline, *N*,*N*-dimethylaniline and *N*,*N*-diethylaniline — a conformational structural analysis using local mode model. Spectrochim. Acta A 60, 351–355.
Silva, A.F., Carvalho, G., Soares, R., Coelho, A.V., Barreto Crespo, M.T., 2012. Step-by-step strategy for protein enrichment and proteome characterisation of extracellular polymeric substances in wastewater treatment systems. Appl. Microbiol. Biotechnol. 95, 767–776.
Ueno, H., Moto, T., Sayato, Y., Nakamuro, K., 1996. Disinfection by-products in the chlorination of organic nitrogen compounds: by-products from kynurenine. Chemosphere 33, 1425–1433.
USEPA, 1995. Method 551.1: Determination of Chlorination Disinfection Byproducts, Chlorinated Solvents, and Halogenated Pesticides/Herbicides in Drinking Water by Liquid-Liquid Extraction and Gas Chromatography with Electron-Capture Detection. Cincinnati, Ohio, US.
USEPA, 2003. Method 552.3: Determination of Haloacetic Acids and Dalapon in Drinking Water by Liquid-Liquid Microextraction, Derivatization, and Gas Chromatography with Electron Capture Detection. Cincinnati, Ohio, US.
Wang, Z.K., Kim, J., Seo, Y., 2012. Influence of bacterial extracellular polymeric substances on the formation of carbonaceous and nitrogenous disinfection byproducts. Environ. Sci. Technol. 46, 11361–11369.
Wang, Z.K., Choi, O., Seo, Y., 2013. Relative contribution of biomolecules in bacterial extracellular polymeric substances to disinfection byproduct formation. Environ. Sci. Technol. 47, 9764–9773.
Wendt, M.A., Meiler, J., Weinhold, F., Farrar, T.C., 2010. Solvent and concentration dependence of the hydroxyl chemical shift of methanol. Mol. Phys. 93, 145–152.
Westerhoff, P., Chao, P., Mash, H., 2004. Reactivity of natural organic matter with aqueous chlorine and bromine. Water Res. 38, 1502–1513.
Wingender, J., Neu, T.R., Flemming, H.C., 1999. Microbial Extracellular Polymeric Substances: Characterization, Structure and Function, Springer, Berlin.
Yang, X., Shen, Q.Q., Guo, W.H., Peng, J.F., Liang, Y.M., 2012. Precursors and nitrogen origins of trichloronitromethane and dichloroacetonitrile during chlorination/chloramination. Chemosphere 88, 25–32.
Zhang, H., Andrews, S.A., 2012. Catalysis of copper corrosion products on chlorine decay and HAA formation in simulated distribution systems. Water Res. 46, 2665–2673.
Zhang, P., Guo, J.S., Shen, Y., Yan, P., Chen, Y.P., Wang, H., Yang, J.X., Fang, F., Li, C., 2015. Microbial communities, extracellular proteomics and polysaccharides: a comparative investigation on biofilm and suspended sludge. Bioresour. Technol. 190, 21–28.